

AO-R198 035

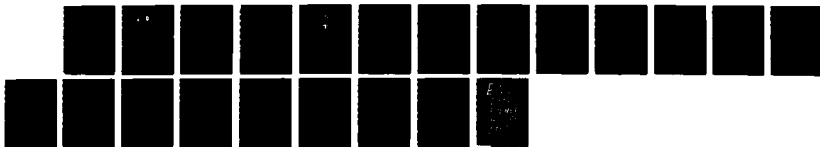
ELECTRONIC ENERGY TRANSFER PROCESSES IN THE  
ALKALI/ALKALINE EARTH METAL VAPORS(U) COLORADO UNIV AT  
BOULDER S R LEONE ET AL 15 JAN 88 AFOSR-TR-88-0167  
AFOSR-84-0272

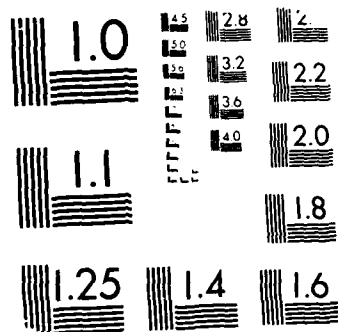
1/1

UNCLASSIFIED

F/G 20/5

NL





MICROCOPY RESOLUTION TEST CHART  
NATIONAL BUREAU OF STANDARDS-1963-A

## REPORT DOCUMENTATION PAGE

**AD-A190 035****TIC  
ELECTE  
D**2b. DECLASSIFICATION/DOWNGRADING SCHEDULE  
**FEB 29 1988**

4. PERFORMING ORGANIZATION REPORT NUMBER(S)

1b. RESTRICTIVE MARKINGS

3. DISTRIBUTION/AVAILABILITY OF REPORT

Approved for public release distribution

5. MONITORING ORGANIZATION REPORT NUMBER(S)

**AFOSR-TR- 88 - 0167**

6a. NAME OF PERFORMING ORGANIZATION

JILA

6b. OFFICE SYMBOL  
(If applicable)

7a. NAME OF MONITORING ORGANIZATION

Air Force Office of  
Scientific Research/NC

6c. ADDRESS (City, State and ZIP Code)

University of Colorado  
Campus Box 440  
Boulder, CO 80309-0440

7b. ADDRESS (City, State and ZIP Code)

Bldg. 410  
Bolling Air Force Base  
Washington, DC 203328a. NAME OF FUNDING/SPONSORING  
ORGANIZATIONAir Force Office of  
Scientific Research8b. OFFICE SYMBOL  
(If applicable)

NC

9. PROCUREMENT INSTRUMENT IDENTIFICATION NUMBER

AFOSR-84-0272

8c. ADDRESS (City, State and ZIP Code)

Bldg. 440  
Bolling Air Force Base  
Washington, DC 20332

10. SOURCE OF FUNDING NOS.

PROGRAM  
ELEMENT NO.PROJECT  
NO.TASK  
NO.WORK UNIT  
NO.

61102F

2303

B1

11. TITLE (Include Security Classification)

Electronic energy transfer processes in the alkali/alkaline earth metal vapors (unclassified)

12. PERSONAL AUTHOR(S)

Stephen R. Leone and Alan C. Gallagher

13a. TYPE OF REPORT

Final report

13b. TIME COVERED

FROM 8/5/84 TO 1/15/88

14. DATE OF REPORT (Yr., Mo., Day)

1988 January 15

15. PAGE COUNT

19

16. SUPPLEMENTARY NOTATION

17. COSATI CODES

FIELD	GROUP	SUB. GR.

18. SUBJECT TERMS (Continue on reverse if necessary and identify by block number)

electronic energy transfer, laser, alkali, alkaline  
earth atoms, metal vapor

19. ABSTRACT (Continue on reverse if necessary and identify by block number)

Collisional energy transfer rates from highly excited  $1p$  states to nearby  $3p$ ,  $1D$ ,  $3D$ , and  $3F$  states of Ca and Sr and fine-structure mixing within the metastable  $3P$  state of Sr have been studied. Several collisional and stimulated population-transfers between the lowest  $1p$ ,  $3p$ ,  $1D$ , and  $3D$  states of Sr have been isolated, and energy-pooling in collisions between pairs of these "energy storage" states has been studied. These processes interconnect the excited-state populations and produce energy leakage during high energy-density storage in these "metastable" states. During the course of these studies, several multiphoton excitation and stimulated Raman population processes have been discovered. Studies have also been carried out to measure the effects of "p" orbital alignment on the cross sections for electronic state-changing collision. Large and remarkably selective alignment effects have been observed for energy transfer processes in both calcium and strontium upon collisions with rare gases and with some molecules, revealing a new level of detail about the precise curve crossings and electronic potentials.

20. DISTRIBUTION/AVAILABILITY OF ABSTRACT

UNCLASSIFIED/UNLIMITED ☐ SAME AS RPT. ☒ OTIC USERS ☐

21. ABSTRACT SECURITY CLASSIFICATION

UNCLASSIFIED

22a. NAME OF RESPONSIBLE INDIVIDUAL

Dr. Francis J. Wodarczyk

22b. TELEPHONE NUMBER  
(Include Area Code)

202-767-4963

22c. OFFICE SYMBOL

NC

Final Report

In the past several years under AFOSR sponsorship, our groups have made unique progress in the study of electronic excitation and energy transfer processes in alkaline earth metal vapors. We have measured cross sections for energy transfer among high-lying electronically excited states of calcium and strontium, induced by buffer-gas collisions. We combine both time-resolved kinetic techniques with emission amplitude measurements to define the absolute rates and pathways. The results have been analyzed in terms of current theoretical methodology to develop propensity rules which describe electronic energy transfer. We have measured J mixing within the metastable  $3P$  states, and collisional and stimulated radiation coupling between the lowest  $1P$ ,  $3P$ ,  $1D$ , and  $3D$  states of Sr. We have measured energy-pooling collisions between several combinations of these low-lying, metastable states of Sr. These have led to major revisions and additions to understanding of high-density energy storage in these metastable states. We have also measured a large array of new orbital alignment effects in electronic energy transfer, to determine the influence of orbital directionality on the cross sections of electronic energy transfer.<sup>1-3</sup> The alignment effects are large, and have been observed both with rare gas and molecular collisions. In several cases, the determinations of these preferential orbital alignment effects are carried out both in the forward and reverse directions, providing a definitive measurement of the symmetry of the potentials involved in the curve crossing. Several highly state-selective effects are also observed, indicating that these orbital alignment determinations provide a remarkable new level of detail on the nature of electronic energy transfer pathways. These results have stimulated new theoretical efforts and important speculation on the quantum mechanics of

electronic energy transfer.<sup>34-36</sup>

Previous studies<sup>4-6</sup> in the group of Leone obtained cross section data for many near resonant energy transfer processes in atomic calcium. These included the study of spin-changing collisions, fine structure changes, and near resonant transfer to states of different configuration. These studies set the stage for much of the recent work on orbital alignment effects. New investigations were carried out during this grant period<sup>o</sup> by R. Schwenz on the electronically excited 6p state of atomic strontium, using similar techniques.<sup>7</sup> This study also provides important collisional transfer rates both for comparison to theory and for development of exciting new experiments on orbital alignment effects, which will be described below. Thus the mapping of the excited state pathways and rates described in this section provides some "bread and butter" measurements necessary for more elegant investigations, such as orbital alignment effects.

A novel cell to contain the Ca or Sr for total cross section measurements, radiative lifetimes, and branching fraction determinations is illustrated in Fig. 1. The cell consists of a sapphire tube held between two heated plates. The Sr metal is contained in a sidearm and can be separately heated to produce a desired vapor pressure. The whole cell is surrounded by an evacuated enclosure. Collisional deactivation partners are introduced through intentional openings. A 5 ns pulsed dye laser is used to excite the Sr vapor to the  $5s6p\ ^1P_1$  state and collisional transfer is observed by detection of fluorescence from various excited states as a function of time after the laser pulse. Individual states are interrogated by using selected interference filters or by resolving the emission with a monochromator. The emission is detected with a fast photomultiplier and a high speed transient digitizer. Results were obtained<sup>7</sup> consisting of cross section and radiative

12/23/80  
AUG 1980

<input checked="" type="checkbox"/>	<input type="checkbox"/>	<input type="checkbox"/>
Codes		
a/or		
al		

A-1

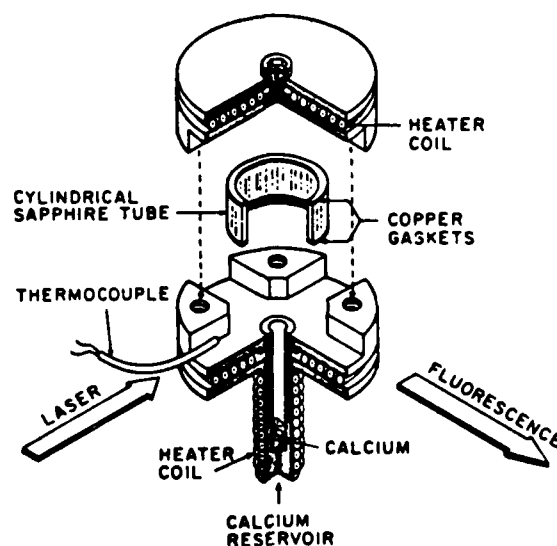


Fig. 1 Cell design for total cross section determinations.

lifetime determinations on the atomic Sr  $6^1P_1$  state and its transfer to the near-resonant  $5p6p^3P_J$ ,  $4d5p^3F_J$ , and  $4d5p^1D_2$  states induced by buffer gas collisions. The total quenching cross sections of the  $^1P$  state are 80, 40, 73, 101, and  $140 \text{ \AA}^2$  for He, Ne, Ar, Kr, and Xe, respectively. The branching fractions into the  $^3P$ ,  $^3F$ , and  $^1D$  states with Kr are 1.0 : 1.3 : 0.3. The accurate radiative lifetime obtained here for the  $^1P$  state is 110 ns, in strong disagreement with determinations by the Hanle effect method.<sup>8</sup> The trend with rare gas is described by a competition between the polarizability interaction, which increases the curve crossing probability for the heavier rare gases, and a velocity effect, which favors more probable transfer for the faster speed of passage through the crossing region, characteristic of the lighter rare gases. The observed branching fractions are explained on the basis of strong mixing of all states in the curve crossing region, at least for collisions induced by Kr. As will be shown below, even though the many near resonant states are heavily mixed in the region of the Sr 6p level and the results of the cross section measurements indicate essentially nearly

statistical branchings, there are remarkably selective effects in the orbital alignment results of this state.

Orbital alignment effects in electronic energy transfer. Effects of alignment and orientation in chemical dynamics comprise an exciting topic of recent investigation.<sup>9,10</sup> A number of chemical reactions have been shown to depend on the alignment of an atomic orbital, including atom transfer processes and associative ionization.<sup>11,12</sup> Thus far, only a few studies have investigated energy transfer processes.<sup>13,14</sup> The effects of charge exchange with aligned excited states have been more thoroughly explored.<sup>15</sup> Some detailed reviews of atomic orbital alignment effects have appeared.<sup>16</sup>

The studies of Bussert, Neuschafer, and Leone<sup>3</sup> are the first to investigate a wide variety of near resonant electronic energy transfer processes in metal vapors, in this case Ca and Sr. This work is also the first to employ pulsed beam and pulsed laser technology for the study of alignment effects. The success of these pulsed laser experiments opens the way for many more studies of this kind because of the broader range of pulsed laser wavelengths available compared to cw lasers. In addition, our work is the first to measure the same energy transfer process in both the forward and reverse directions, from which the dominant symmetry of both potentials involved in the curve crossing is definitively obtained.

Figure 2 shows a schematic of the crossed beam apparatus used for the orbital alignment studies. It consists of an effusive beam of metal vapor, a pulsed beam of target gas, baffle arms to introduce the polarized laser exciting light, and fiber bundles to collect the emission from both the initially excited state and the state that receives the excitation following collision. The signals from both states are digitized and collected for many laser pulses as a function of the angle of polarization of the laser. The

transfer probabilities are normalized for the amount of initial excitation.

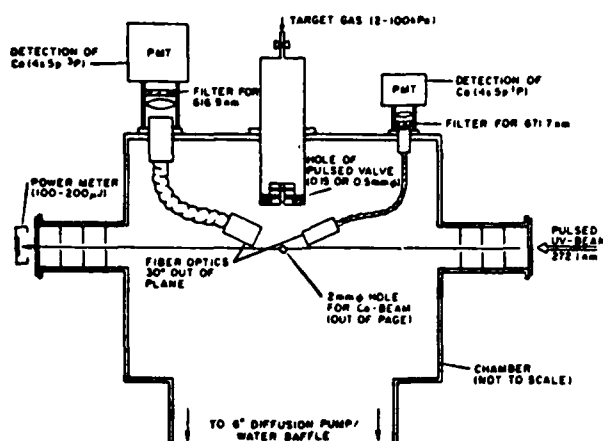


Fig. 2. Schematic of the crossed beam apparatus for alignment experiments.

Since Ca (and effectively Sr) have zero nuclear spin, excitation of the  $^1P$  states with linearly polarized light produces a pure  $m_j$  component which can be related to the orbital electron density. The electronic orbital is aligned along the direction of the laser polarization. The two extreme configurations possible in the center-of-mass reference frame are when the orbital approaches the target gas either parallel or perpendicular to the relative velocity of approach. For the rare gases, this will form the molecular  $\Sigma$  and  $\pi$  states, respectively, in the transient encounter if the initial alignment is retained throughout the collision. The complex interplay involving the details of the degree of retention of the initial alignment, the effects of impact parameter and internuclear separation at the point of curve crossing, the size of the cross section, velocity dependence, and whether the orbital locks into the molecular reference frame are subjects of intense debate.<sup>34-36</sup>

Figure 3 shows a sample of the orbital alignment data for the electronic energy transfer process from Ca  $4s5p\ ^1P_1$  to Ca  $4s5p\ ^3P_1$  induced by He, Xe, and



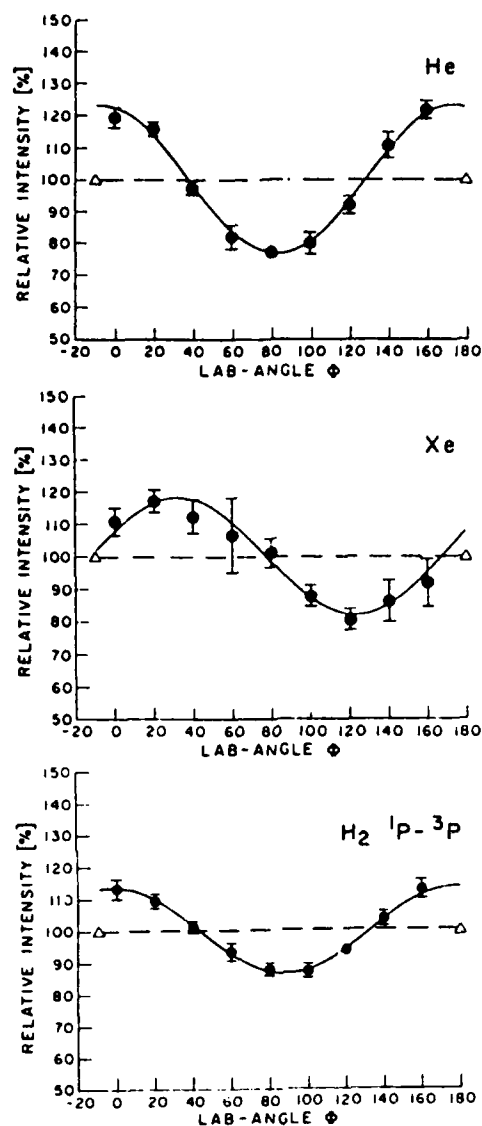


Fig. 3. Dependence of energy transfer cross section on orbital alignment (lab frame angle) in atomic calcium.

$H_2$ . Here the transfer process is confined primarily between these two states because of their strong wave function mixing. The alignment effects for these gases are seen to be large, yielding values of maximum to minimum signal of 1.6, 1.4 and 1.3 for the three gases, respectively. From an analysis of the center-of-mass angle in the collision, it is found that the forward process prefers the  $\pi$  state for He, the  $\Sigma$  state for Xe, and the  $\pi$ -like state for  $H_2$ .

The results of the lighter rare gas, He, and hydrogen can be rationalized on the basis of the simple van der Waals potentials depicted in Fig. 4. Here it is evident that the attraction between the collision partner and the electronically excited Ca is weak, and therefore the well depths of the potentials are similar in magnitude to the splitting of the energy levels.

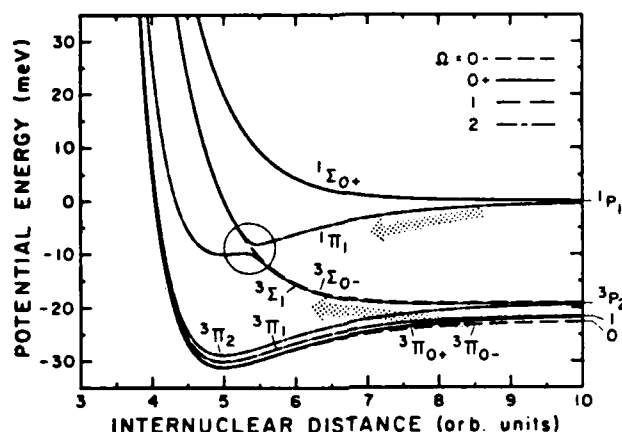


Fig. 4. Schematic potentials for the collision of  $\text{Ca}^* + \text{He}$ . In Ca the  $1P$  and  $3P$  states share an admixture of wave functions, and thus the states are not pure singlets and triplets. Thus an avoided curve crossing can occur between the two states as shown in the figure. The state leading to the crossing in the forward direction is the molecular  $\pi$  state, which is the same state that leads preferentially to the larger cross section in the collisional transfer.

From the curves in Fig. 4, we can make a simple prediction for the effect of the reverse transfer process, that is, if we excite the  $\text{Ca } 3P_1$  state with the linearly polarized laser and let the translational energy in the collision carry the transfer back up to the  $1P$ . Here we would predict that the  $\Sigma$  state should be favored. Because the polarized laser selects the  $m_j$  state, and

since  $J$  is the resultant of the spin and orbital angular momenta, we find that for the same laser polarization, the dominant molecular state is the reverse of the case when the  $^1P$  was excited.<sup>3</sup> Consideration of the coupling schemes that lead to this conclusion is complicated, and involve angular momentum rearrangement as the spin decouples from orbital momentum. This experiment has been carried out with excellent success using the pulsed beam apparatus described. Here we find that whereas the  $\pi$  state is preferred for He in the forward direction, the  $\Sigma$  state is preferred in reverse. A similar result is obtained for  $H_2$ . For Xe, where  $\Sigma$  was preferred in the forward direction, the  $\pi$  state is preferred in reverse. It can be shown by use of the spin-orbit operator that  $\Sigma$ - $\Sigma$  crossings are unlikely, but that the other combinations are possible. Thus in the case of Xe, the  $\pi$  state is the only possibility in the reverse direction. The results for both  $H_2$  and Xe have larger alignment effects in reverse than in the forward direction, perhaps indicating that the effective range of impact parameters is smaller because of the additional endothermicity to reach the actual curve crossing point.

Figure 5 shows all of the data achieved to date for the rare gases as well as numerous molecular collision partners. The results are displayed in terms of the degree of alignment, where a positive alignment in the forward direction favors the perpendicular orbital alignment and a positive alignment in the reverse direction means that the parallel alignment is favored. For the negative alignments, just the reverse is true. The results for Kr and most of the other molecules, except  $H_2$ ,  $D_2$ , and  $CO_2$  do not have a distinguishable alignment effect.

Some very interesting trends and results can be gleaned from the alignment data of Fig. 5. The rare gases seem to show a smooth trend in which

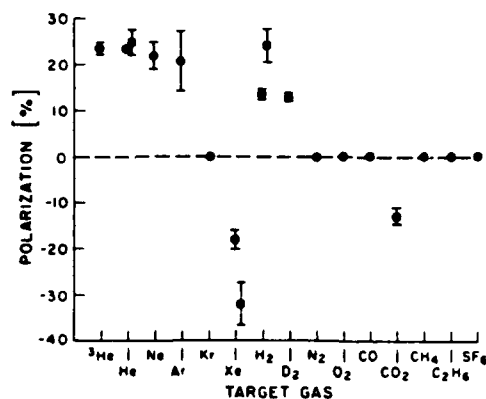


Fig. 5. Alignment data for the Ca  $1p$  to  $3p$  energy transfer. The squares are  $3p$  to  $1p$ .

the lighter masses exhibit a preference for the perpendicular alignment in the forward direction, but the heavier rare gases such as Kr show essentially no effect, and then the effect is reversed for Xe. The reverse processes in the three cases that have been studied so far always show a larger alignment effect than the forward process. The effects for most molecules are negligible or zero, except for hydrogen, deuterium, and carbon dioxide. Part of this may be due to a high reactivity with some molecules, which diminishes the cross section for the energy transfer. The hydrogen species show a strong alignment effect favoring the perpendicular approach, whereas  $\text{CO}_2$  shows a definite preference for the parallel approach. The results, to say the least, show remarkable aspects of state specificity which could not be anticipated.

Further explanation of all the details of the results will require some time for further investigation. The reasons for the difficulty are severalfold. For the heavier rare gases, because of the much deeper potential wells, it is not yet possible to draw the simple potential curves as shown in Fig. 4 for Ca + He. Direct experimental measurements by laser-induced fluorescence on the stable van der Waals molecules for these systems, such as have been carried out for Hg,<sup>17</sup> and recently for Ca, Sr, and Ba,<sup>18</sup> will be the most valuable way to obtain this information, since the calculation of such

most valuable way to obtain this information, since the calculation of such potentials is still difficult. For the molecular collision partners, the availability of numerous molecular orientations in the collision makes the situation considerably more complex.

Nevertheless, it is clear that the results demonstrate some exciting fundamental aspects of the curve crossings and details of electronic energy transfer which have never been obtained before. The complete contrast in the results between atoms such as He, Kr, and Xe and the effects of certain molecules, such as  $\text{CO}_2$ , will provide important challenges for the theoretical interpretation of these effects. Recently, there has been a tremendous surge of interest in these problems theoretically.<sup>19-21</sup> New ideas are being proposed, such as quantum interference effects, which had not previously been associated with these curve crossing phenomena. Our work has provided much of the impetus for these investigations, which are likely to lead to a deeper understanding of electronic energy transfer in general.

As one further example of the elegant state specificity that seems to accompany these new studies of alignment effects, we display in Fig. 6 some very recent data for Sr energy transfer processes. The 6p state of Sr is

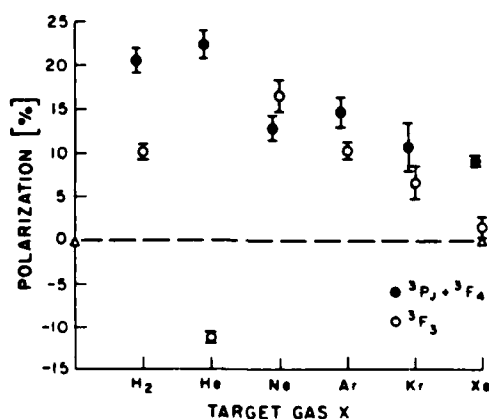


Fig. 6. Alignment data for Sr energy transfer to two states.

analogous to the Ca 5p state; however, in this case, our cross section measurements have shown that three different near resonant states are all populated in the energy transfer. Thus it is possible to interrogate the alignments which access each of several states. This is what is displayed in the figure, in which separate interference filters have been used to resolve the emissions from two states, the  $^3F_2$  and a mixture of  $^3F_4$  and  $^3P_J$  states.

Once again, a remarkable selectivity can be seen in the data. Whereas most of the results fall on a relatively smooth trend with rare gas, showing a perpendicular preference, several points are very different. Helium collisions show the opposite alignment effect for specific population of the  $^3F_2$  state. The trends between the effects for the two different states become reversed from Ne to Xe. New results have now been obtained for several more states in Sr (L.J. Kovalenko). The results are likely to be due to subtle details of the shapes of the potential surface crossings, or perhaps due to the magnitudes of the individual cross sections, and thus will be sensitive to the allowed ranges of impact parameters.

#### Collisional and radiative couplings between low-lying states of Sr.

During the present contract a Nd-YAG pumped dye-laser system was constructed in Gallagher's laboratory for optically pumping metal vapors. This construction and optimization was completed during the first year of the contract, providing lasers pumping in the blue and red wavelength regions, with linewidths of a few times Doppler linewidths and power levels sufficient to saturate most atomic transitions. At the same time a metal-vapor cell with buffer-gas protection of the windows and an associated vacuum and gas-handling apparatus was constructed and tested. Measurements have now been made by pumping the strontium resonance line ( $5\ ^1P_1 - 5\ ^1S_0$ ) with the blue dye laser, and the Sr intercombination transition ( $5\ ^3P_1 - 5\ ^1S_0$ ) with the red dye laser.

To facilitate discussion of these measurements and their current status, we will refer to the strontium energy diagram in Fig. 7. Here the levels being studied are the four lowest multiplets, specifically the  $5^1P$ ,  $5^3P$ ,  $4^1D$ , and  $4^3D$  levels. We have been investigating the collisional and radiative transport of population and energy between these four states and their J sublevels, and we have also studied the energy pooling when pairs of these "metastable" levels collide with each other and produce more highly excited states of strontium. These energy-pooling processes are indicated at the right side of Fig. 7, and for  $5^3P$  as an arrow. The excitation and mixing within the four lowest multiplets is indicated in Fig. 8. These processes will be discussed in more detail in the following.

When the  $5^1P$  level of strontium is strongly excited with a high-power pulsed laser, stimulated Raman radiation transfers population immediately to the  $4^1D$  level, as indicated in Fig. 8. This level is radiatively long-lived and it forms a reservoir of excited population immediately after the 10 ns laser pulse terminates. The population in the  $5^1P$  level would also be "metastable" in high density strontium vapor due to radiation trapping, but in our present experiments very low density strontium vapor is deliberately used in order to diagnose and understand the collisional and radiative processes. Thus, the  $5^1P$  population radiatively decays with a 10 ns lifetime, leaving primarily excited  $4^1D$  population ~50 ns after the laser pulse. As indicated in Fig. 8, buffer-gas collisional transfer then occurs from this large population initially in the  $4^1D$  state to the  $4^3D$  and the  $5^1P$  states. The  $4^3D$  state then radiatively decays to  $5^3P$ , which radiates slowly to the ground state (in 20-50  $\mu$ s). Only one of the three J levels of  $5^3P$  actually radiates to the ground state, so that J mixing is also an important term in the time dependent behavior of the excited population. The overall result of

these various steps is a typical excited-state storage time of  $\sim 100 \mu\text{s}$ , but spread through several states and with complicated time behavior and stimulated emission. For example, stimulated emission can also occur from  $5^1P_1$  to the  $4^3D$  state and from there to the  $5^3P$  levels at high Sr density, as these are not pure triplet states and intercombination radiation can occur.

In our measurements we have diagnosed the time-dependent fluorescence of the  $5^1P$  and  $5^3P_1$  levels, as well as the populations of the  $5^3P_0$  and  $5^3P_2$  levels by absorption to higher states. As we apply this absorption method to the  $4^1D$  and  $4^3D$  levels as well, we can also follow their time-dependent populations. Here we use absorption of Sr lines from a hollow-cathode lamp, propagating through the cell perpendicular to the laser, and we adjust the

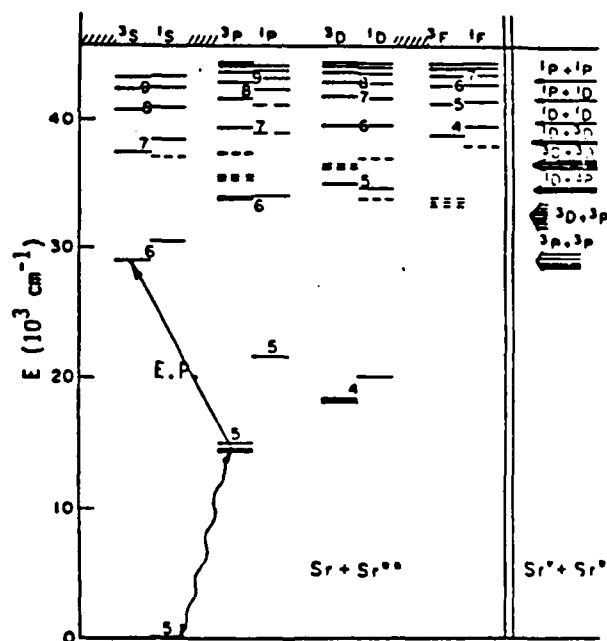


Fig. 7. Sr energy levels, with those of predominately  $(5s \ nL)$  configuration as solid lines and of other configurations as dashed lines. Energy-pooling due to various pairs of "metastable" states is indicated on the right, and the example of  $5^3P_1$  excitation followed by  $5^3P + 5^3P \rightarrow 6^3S_0 + 5^1S_0$  is shown with arrows.



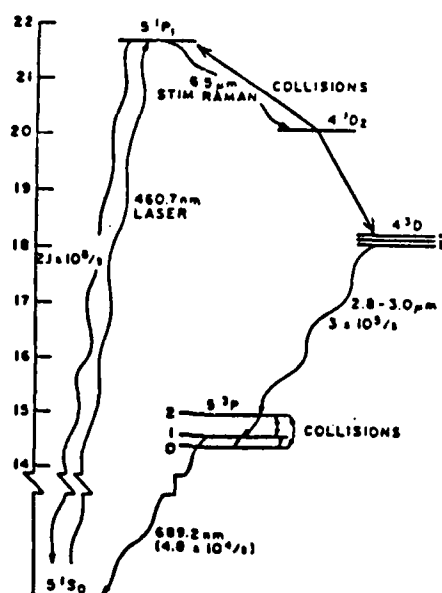


Fig. 8. Collisional and radiative processes that result from saturating the Sr resonance line ( $5^1P_1$ - $5^1S_0$ ).

strontium density until we have excited-state densities in the neighborhood of  $10^{10} \text{ cm}^{-3}$  to provide an appropriate absorption signal. From these time-dependent fluorescent and absorption measurements following  $5^1P$  excitation, we have deduced several of the stimulated Raman processes, as well as the collisional transfer processes due to inert gas collisions. The mixing between these four levels, which are effectively all metastable in a high pressure strontium gas, are the very processes which determine their populations and the ability to store energy in these levels under high-power excitation conditions. Rate coefficients for these collisional energy transfers have been determined for several of the transitions.<sup>22</sup> We note here that these collisional transitions occur within the same spin multiplet as well as between multiplets with different spin labeling. However, in the latter case none of these states under consideration are pure spin states, and

as a result the inter-multiplet radiation and collisional transitions can be explained by the mixed-spin character of these states.

Fine-structure mixing. In a second set of measurements we have optically pumped the  $5^3P_1$  state at the same strontium densities of  $10^{10}$ - $10^{11}$   $\text{cm}^{-3}$  (see Fig. 7). We then observe the time-dependent population of  $5^3P_0$ ,  $5^3P_1$ , and  $5^3P_2$  states that result from collisional mixing, by absorbing from these levels to the  $6^3S_1$  state and by monitoring the 689.2 nm radiation fluorescence of the  $5^3P_1$  level. An example of these time-dependent populations is shown in Fig. 9. From these observations we have obtained the collisional mixing rates between these fine-structure levels. Contrary to previous literature<sup>23,24</sup> these are very low mixing rate coefficients in the heavy inert gas buffers, typically  $10^{-4}$  of gas kinetic rates.<sup>25</sup> On the other hand, the mixing is rapid in molecular buffers, and we believe that the observations reported in Ref. 23 are influenced by the presence of small fractions of molecular impurities in their inert gases.

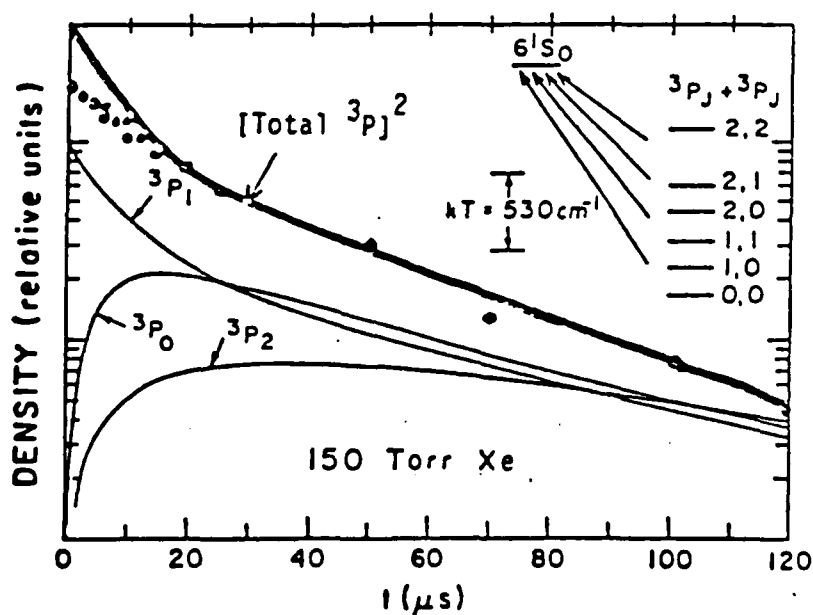


Fig. 9. The  $5^3P_J$  level populations following  $5^3P_1$  excitation at  $t=0$ . The  $6^1S_0$  production rate (dots) due to energy-pooling collisions of pairs of  $5^3P$  states is compared to the square of the total  $5^3P$  density (line). The difference is due to  $J$  dependences of the collisional rate coefficients.

Energy-pooling collisions. In the next set of measurements we have measured energy pooling from the  $5\ ^3P_J$  levels to the  $6\ ^3S_1$  and  $6\ ^1S_0$  levels following optical excitation of the  $5\ ^3P_1$  level, as shown diagrammatically in Figs. 7 and 9. By saturating the  $5\ ^3P_1$  state excitation and measuring the initial strontium density (by resonance line absorption), we have established the exact density of the  $5\ ^3P_1$  level, and thereby of all the  $5\ ^3P_J$  levels responsible for the energy pooling. Thus we can reduce our data to obtain quantitative rate coefficients for this process.<sup>26</sup> We find that these energy-pooling rate coefficients are very large ( $10^{-10}$ - $10^{-9}\ \text{cm}^3\ \text{s}^{-1}$ ), particularly to the  $6\ ^3S_1$  state, whereas the energy defect between the pair-excited states and the singly excited states vary from  $30$ - $500\ \text{cm}^{-1}$ . Thus, this represents a very major energy loss mechanism in any storage system. Indeed, this is probably the largest single energy loss term and therefore sets the limit for the density of energy that can be stored in these states. We are in the process of studying energy pooling by collisions of other pairs of the  $5\ ^1P$ ,  $4\ ^1D$ ,  $4\ ^3D$ , and  $5\ ^3P$  levels. Some of these may have smaller energy-pooling rate coefficients, allowing somewhat greater energy storage density, but this is not established at the present time.

Off-resonant, two-photon excitation. In the process of these measurements we have also discovered an unexpected and extremely efficient method of producing a very large density of highly excited strontium atoms. Its consequence is that a large percentage of ground state strontium atoms can be pumped into the  $9\ ^1P$  and  $10\ ^1S$  levels of strontium during a  $10\ \text{ns}$  laser pulsed tuned to the resonance transition. As shown in Fig. 7, when this resonance transition is saturated, a second laser photon can excite from  $5\ ^1P$  within  $100\ \text{cm}^{-1}$  of the  $10\ ^1S$  and  $9\ ^1P$  levels. This  $100\ \text{cm}^{-1}$  detuning would normally be expected to preclude significant radiative excitation to these

higher levels, but we find that in the presence of buffer gas a very high population transfer occurs, far greater than expected on the basis of normal collisional-line-broadening absorption. We suspect this is related to stimulated Raman processes with photon wavelengths in the 100 wavenumber region, but this is currently under study in order to obtain a definitive explanation. We are not aware of any literature regarding such collision-induced stimulated processes into highly excited states, but as this could be a very important excitation and radiative loss mechanism in high power laser gases we are investigating it further.

The  $5^3P_J$  fine-structure collisional mixing experiment is essentially completed and a publication is in preparation reporting these results.<sup>25</sup> Here we have found a very surprising pressure dependence for some of these mixing rate coefficients, implying a very large three-body collisional contribution in the cases of the heavier rare gases. Such a three-body atomic collisional transfer may not have been previously observed, as it may be unique to this situation of a nearly-forbidden 2-body transfer (due to adiabaticity for this large fine-structure splitting), plus the metastable character of the levels which allows a long time for excited-molecule formation. The 2-body rate coefficients are  $\sim 10^{-15} \text{ cm}^3 \text{ s}^{-1}$  for the heavier rare gases, increasing to nearly  $10^{-9} \text{ cm}^3 \text{ s}^{-1}$  in the case of a helium buffer due to the much faster velocity of the helium. The three-body J-mixing rate coefficients are  $\sim 10^{-33} \text{ cm}^6 \text{ s}^{-1}$ , probably due to a three-body process for forming a stable diatomic, followed by a J change accompanied by dissociation.

### References

1. M.O. Hale, I.V. Hertel and S.R. Leone, Phys. Rev. Lett. 53, 2296 (1984).
2. D. Neuschafer, M.O. Hale, I.V. Hertel and S.R. Leone, in Electronic and Atomic Collisions, Eds. D.C. Lorents, W.E. Meyerhof and J.R. Petersen (Elsevier, Amsterdam, 1986), pp. 585-591.
3. W. Bussert, D. Neuschafer and S.R. Leone J. Chem. Phys. 87, 3833 (1987).  
W. Bussert and S.R. Leone, Chem. Phys. Lett. 138, 269, 276 (1987).
4. W.H. Pence and S.R. Leone, J. Chem. Phys. 74, 5707 (1981).
5. M.O. Hale and S.R. Leone, J. Chem. Phys. 79, 3352 (1983).
6. M.O. Hale and S.R. Leone, Phys. Rev. A31, 103 (1985).
7. R.W. Schwenz and S.R. Leone, Chem. Phys. Lett. 133, 433 (1987).
8. F.M. Kelly, T.K. Koh and M.S. Mathur, Can. J. Phys. 53, 930 (1975).
9. R.N. Zare, Ber. Bunsenges, Phys. Chem. 86, 422 (1982), and review of other work therein.
10. S. Stolte, Ber. Bunsenges, Phys. Chem. 86, 413 (1982), and review of other work therein.
11. T. Rettner and R.N. Zare, J. Chem. Phys. 77, 2416 (1982).
12. M-X. Wang, M.S. deVries and J. Weiner, Phys. Rev. A33, 765 1612 (1986),  
H.A.J. Meijer, H.P. v.d. Meulen, R. Morgenstern, I.V. Hertel, E. Meyer,  
H. Schmidt and R. Witte, Phys. Rev. A33, 1421 (1986).
13. M.P.I. Manders, J.P.J. Priessen, H.C.W. Beijerinck and B.J. Verhaar,  
Phys. Rev. Lett. 57, 1577 (1986).
14. W. Bussert, T. Bregel, R.J. Allan, M.W. Ruf and H. Hotop, Z. Phys. A320, 105 (1985).
15. A. Bahring, I.V. Hertel, E. Meyer and H. Schmidt, Phys. Rev. Lett. 53, 1433 (1984).
16. I.V. Hertel, H. Schmidt, A. Bahring and E. Meyer, Rep. Prog. Phys. 48, 375 (1985).
17. K. Yamanouchi, J. Fukuyama, H. Horiguchi, S. Tsuchiya, K. Fuke, T. Saito and K. Kaya, J. Chem. Phys. 85, 1806 (1986), and B. Soup, private communication.
18. A. Kowalski, D.J. Funk, and W.H. Breckenridge, Chem. Phys. Lett. 132, 263 (1986).
19. A.Z. Devdariani and A.L. Zagrebin, Chem. Phys. Lett. 131, 197 (1986).

20. B. Pouilly and M.H. Alexander, J. Chem. Phys. 86, 4790 (1987).
21. I.V. Hertel, R. Witte and E.E.B. Campbell, private communication.
22. Some details of these measurements were reported at the contractors conference at AFCRL, October 19, 1985.
23. D. Husain and J. Schifino, J. Chem. Far. Trans. 80, 321 (1984).
24. J.J. Wright and L.C. Balling, J. Chem. Phys. 73, 1617 (1980).
25. J. Kelly, M. Harris, and A. Gallagher, Phys. Rev. A (submitted)
26. M. Harris, J. Kelly, and A. Gallagher, Phys. Rev. A 36, 1512 (1987).

END

DATE

FILMED

4-88

DTIC